The Astrophysical Journal, 875:88 (8pp), 2019 April 20 https://doi.org/10.3847/1538-4357/ab1006

A Discovery of Young Radio Sources in the Cores of Giant Radio Galaxies Selected at Hard X-Rays

G. Bruni[1], F. Panessa[1], L. Bassani[2], E. Chiaraluce[1,3], A. Kraus[4], D. Dallacasa[5,6], A. Bazzano[1], L. Hernández-García[7], A. Malizia[2], P. Ubertini[1], F. Ursini[2], and T. Venturi[6]
[1] INAF—Istituto di Astrofisica e Planetologia Spaziali, via Fosso del Cavaliere 100, I-00133 Roma, Italy; gabriele.bruni@inaf.it
[2] INAF—Osservatorio di Astrofisica e Scienza dello Spazio di Bologna, Via Piero Gobetti 93/3, I-40129 Bologna, Italy
[3] Dipartimento di Fisica, Universitá di Roma Tor Vergata, via della Ricerca Scientifica 1, I-00133 Roma, Italy
[4] MPIfR—Max Planck Institute for Radio Astronomy, auf dem Hügel 69, D-53121 Bonn, Germany
[5] DiFA—Dipartimento di Fisica e Astronomia, Universitá di Bologna, via P. Gobetti 93/2, I-40129 Bologna, Italy
[6] INAF—Istituto di Radioastronomia, via Piero Gobetti 101, I-40129 Bologna, Italy
[7] IFA—Instituto de Física y Astronomía, Facultad de Ciencias, Universidad de Valparaíso, Gran Bretaña 1111, Playa Ancha, Valparaíso, Chile
Received 2018 November 29; revised 2019 March 6; accepted 2019 March 13; published 2019 April 19

Abstract

Giant radio galaxies (GRG) are the largest single entities in the universe, having a projected linear size exceeding 0.7 Mpc, which implies that they are also quite old objects. They are not common, representing a fraction of only ∼6% in samples of bright radio galaxies. While a census of about 300 of these objects has been built in the past years, still no light has been shed on the conditions necessary to allow such an exceptional growth, whether of environmental nature or linked to the inner accretion properties. Recent studies found that samples of radio galaxies selected from hard X-ray active galactic nuclei catalogs selected from the *International Gamma-Ray Astrophysics Laboratory* (*INTEGRAL*)/the Imager on Board the *INTEGRAL* Satellite and *Swift*/the Burst Alert Telescope (thus at energies >20 keV) present a fraction of GRG four times larger than what is found in radio-selected samples. We present radio observations of 15 nuclei of hard-X-ray-selected GRG, finding for the first time a large fraction (61%) of young radio sources at the center of Mpc-scale structures. Being at the center of GRG, these young nuclei may be undergoing a restarting activity episode, suggesting a link between the detected hard X-ray emission—due to the ongoing accretion—and the reactivation of the jets.

Key words: galaxies: active – galaxies: jets – galaxies: nuclei – radio continuum: galaxies – X-rays: galaxies

1. Introduction

A fraction of radio galaxies (∼6% in the revised version of the third Cambridge catalog of radio sources (3CR); Ishwara-Chandra & Saikia 1999) exhibits exceptional projected linear extents, i.e., above 0.7 Mpc, making them the largest individual objects in the universe. Both Fanaroff–Riley type I and type II radio galaxies (FRI and FRII respectively; Fanaroff & Riley 1974) are represented in samples of giant radio galaxies (GRG). While FRI GRG are associated with early-type galaxies, those with FRII morphology are hosted both in early-type galaxies and quasars. Despite the overall uncertainties underlying the assumption that spectral ages of radio galaxies are representative of their dynamical ages (Parma et al. 1999), it seems plausible that GRG are, on average, very old radio sources, with radiative ages between 10^7 and 10^8 yr (Machalski et al. 2004; Jamrozy et al. 2008). Nevertheless, it is still under debate whether their extreme size is due to the core/accretion properties, possibly with more than one activity episode (Subrahmanyan et al. 1996); to a convenient environment conditions, with GRG expanding in a low-density intergalactic medium (IGM; Marecki 2004); or to a combination of both effects. A more recent study using a population of hundreds of objects, and spanning different cosmic epochs ($0.016 < z < 3.22$), seems to exclude a main role of IGM in the expansion of the lobes (Kuźmicz et al. 2018), failing in finding a significant match of GRG with cosmic voids.

On the other end of radio galaxies evolution, nearly 8.5÷10% of radio sources from surveys at kpc-scale resolution present a spectral shape peaking in the MHz–GHz frequency range (O'Dea 1998). Considered to be the young precursors of FRI and FRII radio galaxies, they were divided into three classes depending on the synchrotron peaking range: compact steep spectrum sources (CSS; Fanti et al. 1990), peaking at frequencies <500 MHz; gigahertz peaked spectrum sources (GPS; O'Dea et al. 1991), peaking between 500 MHz and a few GHz; and high-frequency peakers (HFP; Dallacasa et al. 2000), peaking at frequencies higher than ∼5 GHz. An anticorrelation between the linear size and peaking frequency was found for the three groups, due to synchrotron self absorption, and spanning a scale between 1 and 20 kpc for CSS, less than 1 kpc for GPS, and less than 100 pc for HFP (O'Dea 1998; Dallacasa 2003). This suggests an evolutionary track from HFP to CSS, due to the expansion of plasma within the interstellar medium of the host galaxy. Further support to this scenario was given by Very Long Baseline Interferometry (VLBI) observations with a pc-scale angular resolution, revealing typical morphologies of twin lobed objects, sometimes with a weak central nucleus, similar to what is found for larger and older radio galaxies. Jets and nuclei are more prominent in compact steep spectrum quasars (Phillips & Mutel 1980; Wilkinson et al. 1994; Stanghellini et al. 1997; Orienti et al. 2006). Estimates of the kinematic age for the most compact sources have revealed an age of below ∼10 kyr (Owsianik & Conway 1998), as also confirmed by radiative aging estimates (Murgia et al. 1999). Another long-debated scenario, which eventually did not find sufficient support from observations, tried to explain the compact size as a consequence of a dense medium, frustrating the expansion of the jets (van Breugel et al. 1984; Bicknell et al. 1997).

Finding one of these sources at the center of a GRG would imply that the core is undergoing an event that retriggered the radio activity, since the Mpc-scale structure suggests a previous expansion phase that lasted a few hundreds of Myr at least. With this work, we aim at testing the presence of young radio components in the core of a hard-X-ray-selected sample of GRG in order to estimate the fraction of such objects with a signature of restarting radio activity.

2. The Hard-X-Ray-selected GRG Sample

This work is part of our ongoing multi-wavelength study of a sample of hard-X-ray-selected GRG. Bassani et al. (2016) performed a combined radio/hard X-ray study of the active galactic nuclei (AGN) population selected in the hard X-ray band by the *International Gamma-Ray Astrophysics Laboratory* (*INTEGRAL*)/the Imager on Board the *INTEGRAL* Satellite (IBIS) and *Swift*/the Burst Alert Telescope (BAT) surveys, finding 64 objects that match radio galaxies with known redshifts. The NRAO Very Large Array (VLA) Sky Survey (NVSS) and Sydney University Molonglo Sky Survey (SUMSS) maps allowed an estimate of the projected linear size, and it turned out that 14 of them (i.e., ∼25% of the sample) can be classified as GRG. Considering the overall fraction of giant sources in samples of radio galaxies—e.g., ∼6% in the 3CR catalog (Ishwara-Chandra & Saikia 1999) and 8% in the 3CRR sample (Laing et al. 1983)—this fraction is impressively large and suggests a connection between the nuclear properties and the evolution of the radio structure up to the Mpc scale. Nevertheless, the same authors do not exclude that an observational bias, due to the hard X-ray selection, could affect the GRG fraction estimate in their work.

Since 2014, we have been carrying out an observing campaign on these 14 GRG, aiming at testing the physical conditions in these peculiar sources. From Giant Metrewave Radio Telescope (GMRT) data at 325 MHz on a subsample of four objects, we could find two newly discovered GRG (IGR J14488-4008, Molina et al. 2015; IGR J17488-2338, Molina et al. 2014). From a VLBI follow-up, another source showed clear signs of an extreme reorientation (PBC J2333.9-2343; Hernández-García et al. 2017), which is also possibly connected to restarted activity. Finally, Ursini et al. (2018) presented a study of the X-ray versus radio luminosity properties; interestingly enough, the radio luminosity of the lobes is lower than what is expected from the core one, assuming that the actual core luminosity was the same for all of the source lifetime. This may suggest recently restarted nuclear activity. These results pointed toward the importance of a study of the core components of these GRG, aiming at finding possible differences with respect to common radio galaxies. In this work, we present the radio spectra from 150 MHz to 10 GHz of the 14 GRG of the sample, plus an additional source (B2 1144+35B) from the latest *INTEGRAL*/IBIS AGN catalog (Malizia et al. 2016).

3. Radio Observations and Ancillary Data

In the following, we present radio flux densities for the cores of our GRG sample collected during our observing campaign at the Effelsberg 100-m single dish telescope, as well as from previous surveys, archives, and works in the literature.

Table 1
Used Receivers of the Effelsberg 100-m Telescope

	S60mm	S36mm	S28mm
Center frequency	4.85 GHz	8.35 GHz	10.45 GHz
Typical T_{sys} (zenith)	25 K	22 K	50 K
HPBW	145 arcsec	82 arcsec	66 arcsec
Sensitivity	1.55 K Jy^{-1}	1.35 K Jy^{-1}	1.35 K Jy^{-1}
No. of pixels	2	1	2

3.1. Effelsberg 100-m Single Dish Telescope Observations

Observations with the Effelsberg 100-m single dish telescope were conducted from 2018 March to July with three secondary focus receivers: S60 mm, S36 mm, and S28 mm—see Table 1 for details. At the lowest frequency (4.8 GHz), the observations were done with on-the-fly (OTF) maps, in order to be able to discriminate the core emission from the extended structure during the data analysis. At 8.5 and 10.5 GHz, the sources were observed by cross-scans over the core position (in azimuth and elevation), conveniently choosing the position angle in order to avoid the jets' and lobes' emission. Data reduction was performed with the `TOOLBOX2`[8] software; for the reduction of the OTF maps, the `NOD3` package was used in addition (Müller et al. 2017). In case of the maps, the first step of the data reduction was a baseline correction and the application of the `Restore` algorithm to combine the data of the two receiver pixels (feeds). The antenna temperature of the cross-scans were determined by a Gaussian fit to the observed pattern, a correction for the (usually small) pointing offset, and by averaging the amplitudes from all subscans. In both cases, further corrections were made for atmospheric attenuation and the gain-elevation effect of the antenna. Finally, the observed antenna temperatures were converted into the absolute flux density scale by comparing with observations of suitable calibrators like 3C286, etc. (using the scale of Baars et al. 1977). Finally, we extracted the core flux density by means of a single-component Gaussian fitting on the images.

3.2. Data from Surveys and Archives

In addition to the Effelsberg data, we also collected measurements from surveys at lower frequencies. In particular, we made use of the recently published TIFR GMRT Sky Survey at 150 MHz (TGSS; Intema et al. 2017), the Westerbork Northern Sky Survey at 325 MHz (WENSS; Rengelink et al. 1997), the SUMSS at 843 MHz (Mauch et al. 2003), and the NVSS at 1.4 GHz (Condon et al. 1998). Due to the extended emission at low frequencies, the different angular resolution can be an issue when trying to measure the core flux density. In general, we refer to the "core region" as the unresolved central component visible at the center of each radio galaxy on scales of tens of arcsec at most, which can be easily disentangled from the remainder of the radio source (i.e., lobes and hot spots). This becomes more and more difficult at low frequencies given the progressively worse angular resolution and the generally flat or even inverted spectrum of such components. Thus, we only considered the data when radio sources were resolved enough to allow good core identification, also comparing WENSS, TGSS, and NVSS. At higher frequencies, the core dominates the emission, thus this is not an issue. For one

[8] https://eff100mwiki.mpifr-bonn.mpg.de/doku.php

southern source (PKS 2014−55), we report the SUMSS flux density for the core region, although we do not consider it when building the spectral shape, since the core is known to be resolved at higher resolution with the Australia Telescope Compact Array (ATCA; see Section 3.3).

We also browsed the NRAO VLA Archive Survey (NVAS; Crossley et al. 2008) looking for archive images of our sources and found data for two of them: 4C +63.22 (23.4 ± 1.1 mJy at 1.4 GHz and 14.3 ± 0.7 mJy at 4.5 GHz) and 4C +34.47 (338 ± 17 mJy at 4.8 GHz, and two epochs at 15 GHz with 767 ± 38 mJy and 226 ± 11 mJy). Finally, for Mrk 1498, we analyzed also the Jansky Very Large Array (JVLA) archive data from 2015; since the full bandwidth of these observations was 4 GHz (spanning the observing frequency from 4 to 8 GHz), we split that into four measurements of 1 GHz bandwidth each in order to increase the frequency coverage. The resulting flux densities are: 130 ± 13 mJy at 4.5 GHz, 127 ± 13 mJy at 5.5 GHz, 125 ± 12 mJy at 6.5 GHz, and 124 ± 12 mJy at 7.5 GHz. A dedicated paper on this source, presenting these JVLA data in more details, is in progress (L. Hernández-García et al. 2019, in preparation).

3.3. Data from the Literature

For six sources, we could also find data in the literature at a suitable angular resolution to discriminate the core from the extended structure. We used the data to improve the spectral coverage and ease flux density peak identification. These are:

1. *PKS 0707-35*. The source was previously studied by Saripalli et al. (2013), who presented ATCA images at 1.4 GHz and 2.3 GHz. The flux densities reported for the core are 44.6 mJy and 53 mJy, respectively, with an inverted spectral index of $\alpha = 0.44$ (adopting the convention $S = \nu^{\alpha}$, where S is the flux density, ν is the frequency, and α is the spectral index). We use these two points, together with TGSS observations, to draw the spectral shape from 150 MHz to 2.3 GHz, finding no peak in this range. Given the low decl. of this source, it was not possible to observe it from Effelsberg, and no data from the main radio surveys are present.
2. *B2 1144+35B*. Multi-epoch VLA data, from 1.4 GHz to 43 GHz, for the arcsec core of this target have been presented in Giovannini et al. (1999, 2007). A substantial flux density variability has been found, with a steady brightening from 1974 to 1992, followed by a dimming at all frequencies from 1992 to 2006. Those authors suggest that the interaction with the external medium could be the most probable scenario to explain the variability over three decades. In Figure 1, we present data for all of the available VLA epochs with more than two frequencies, plus the ones taken in Effelsberg, showing again flux densities lower than the previous ones and confirming the decreasing trend. In addition to that, we report also TGSS and NVSS data, with the latter being taken when the core flux density was at its relative maximum.
3. *IGR J14488-4008*. We observed this source at 325 MHz and 610 MHz during our GMRT campaign in 2014, in which results were partially published (only the 610 MHz image) in Molina et al. (2014) Here, we report the two flux densities (18.8 ± 1.9 mJy at 325 MHz and 32.3 ± 1.3 mJy at 610 MHz), where the first one was extracted from the corresponding map to be presented in a future paper (G. Bruni et al. 2019, in preparation). In addition to this, we also report the flux densities at 5 and 8 GHz from the Australia Telescope-PMN(ATPMN) southern hemisphere survey, carried out with ATCA (McConnell et al. 2012).
4. *PKS 2014-55*. Flux densities at 4.8 GHz and 8.6 GHz from ATCA observations (25.21 ± 0.07 mJy and 20.2 ± 0.05 mJy, respectively) for this source were provided by L. Saripalli (2019, private communication), following the work presented in Saripalli (2007). These values, together with the SUMSS measurements presented in Table 2, are the only data available for this source.
5. *4C +74.26*. Pearson et al. (1992) presented a multi-frequency VLA study of this source's nucleus, from 0.3 to 15 GHz, plus an additional point at 270 GHz from Riley et al. (1989). A clear GPS spectrum is visible, peaking at about 8 GHz. Previous measurements from the literature are fully compatible with the ones collected during our campaign. In addition to these, we also plot the point at 150 MHz from TGSS, which shows a turn-up of the spectrum at low frequencies.
6. *PKS 2331-240*. A study of this source was presented in Hernández-García et al. (2017, 2018), showing that a Blazar-like nucleus is present, implying a dramatic change of the jet axis with respect to the GRG structure likely on the plane of the sky. In Figure 1, we report the data presented in that work, in addition to the ones collected here. The flux density discrepancy at low frequencies (∼150 MHz) is due to the better angular resolution of TGSS with respect to the Galactic and Extragalactic All-sky MWA survey (GLEAM). As suggested by those authors, restarting activity is the most probable scenario for this source, although there is no evidence of the time when it happened. This is in agreement with Callingham et al. (2017), who presented the source as restarting, given the convex radio spectrum (see Section 4 for a discussion of their work).
7. *PKS 2356-61*. This source has a too low decl. for Effelsberg observations. We present the measurement at 1.4 GHz, published in Ursini et al. (2018), and two ATCA measurements at 2.3 GHz and 5 GHz from Morganti et al. (1993, 1997) of 20.5 ± 2.0 mJy and 35.0 ± 3.5 mJy, respectively.

4. Spectral Shapes and Young Radio Sources' Fraction

With the data described in the previous section, we were able to reconstruct the radio spectral shape of the 15 sources of the sample, searching for the presence of a peak in the MHz–GHz frequency range. We have been able to gather at least three flux density measurements for 13 out of the 15 sources, allowing us to constrain the shape, at least in the GHz range, for the majority of them. In order to establish whether or not a GPS peak was present in the radio spectra of these sources, we performed a basic modeling of the data using a log-parabola as a simplified synchrotron emission component, analogously to previous works in the literature (Bruni et al. 2012; Tuccillo et al. 2017). The procedure has the sole purpose of identifying the presence of a peak and not to characterize the different free parameters of the synchrotron components expected from a core spectrum (for which a better sampling would be required).

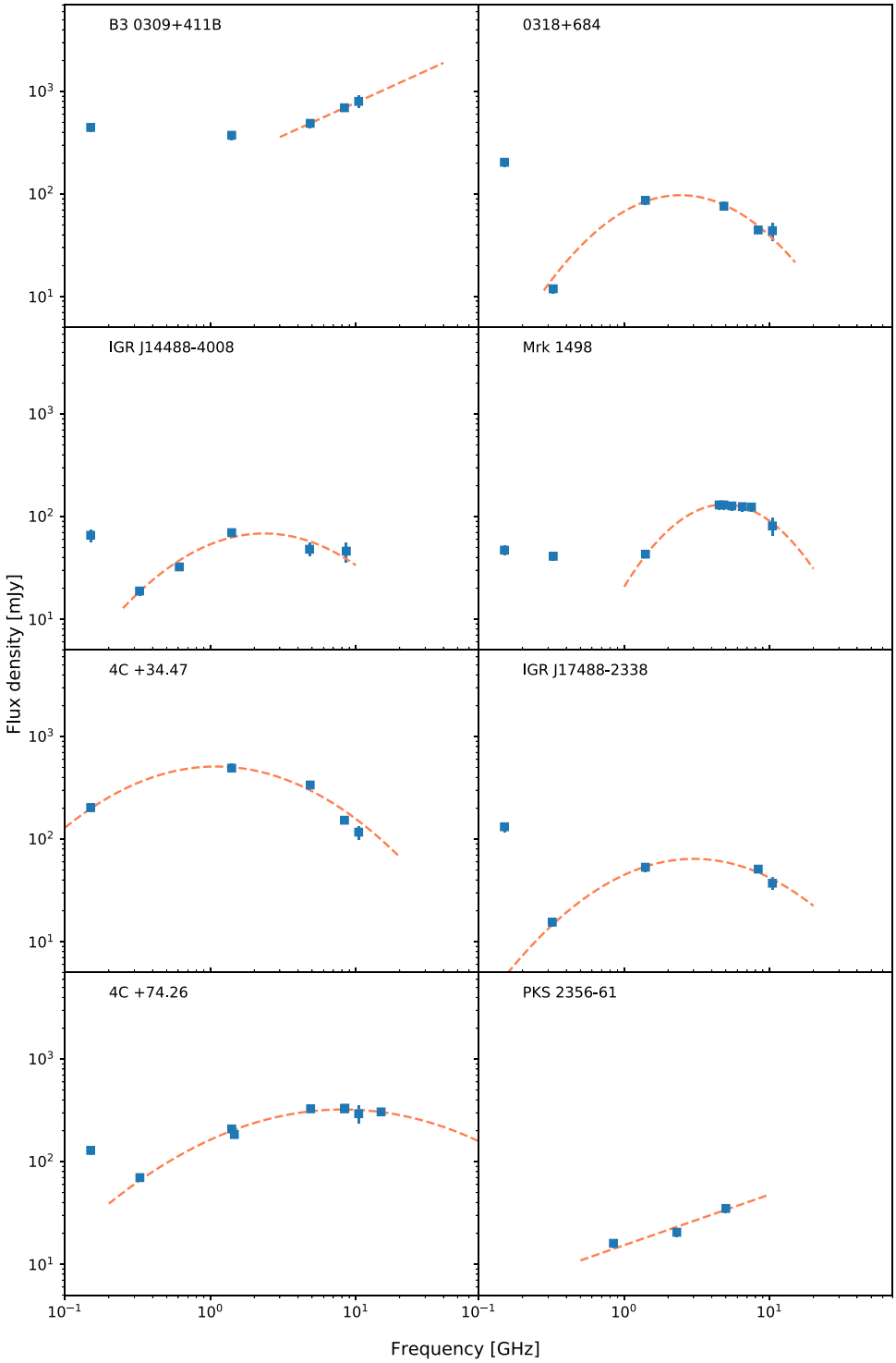

Figure 1. GPS radio cores spectra. Errors in the logarithmic scale are smaller than the symbol size for most measurements. The point at 250 GHz for 4C +74.26 is out of scale.

In particular, we fitted the data with the Astropy `LogParabola1D` function (Astropy Collaboration et al. 2018), using the `LevMarLSQFitter` routine that performs a Levenberg–Marquardt and least squares statistic. We excluded the points that were obviously part of a secondary, older, synchrotron component at low frequencies from the fitting procedure (see below for a discussion). We obtained a good fit for six objects (0318+684, IGR J14488-4008, Mrk 1498, 4C +34.47, IGR J17488-2338, and 4C +74.26). For B3 0309+411B and PKS 2356-61, data above 1 GHz show an inverted spectrum, possibly indicating a self-synchrotron absorption, that could be fitted by a power-law with spectral index of $\alpha = 0.6$ and $\alpha = 0.5$ respectively (using the `PowerLaw1D` function), so we can assume a peak may be present at tens of GHz, which is beyond the spectral window sampled in this work. These could well be examples of HFP sources, thus even younger than the GPS ones. The peak frequency for the modeled GPS components are given in Table 2. Four sources among the

Table 2
List of Collected Flux Densities (in mJy) at Different Frequencies (in GHz) for the Cores of the 15 GRG of Our Sample

Source ID	$S_{0.150}$ (mJy)	$S_{0.325}$ (mJy)	$S_{1.4}$ (mJy)	Effelsberg 100-m			ν_{peak} (GHz)
				$S_{4.8}$ (mJy)	$S_{8.5}$ (mJy)	$S_{10.5}$ (mJy)	
B3 0309+411B	446 ± 45	···	374 ± 37	489 ± 49	694 ± 15	801 ± 111	>10
J0318+684	204 ± 20	12 ± 1	86.8 ± 8.7	76 ± 8	45 ± 2	44 ± 9	2.4
PKS 0707-35	45 ± 5	···	44 ± 4†	···	···	···	···
4C 73.08	···	···	14.5 ± 1.6	10 ± 1	···	11 ± 2	···
B2 1144+35B	368 ± 37	658 ± 66	···	···	169 ± 4	164 ± 24	···
HE 1434-1600	···	···	75.0 ± 7.5	56 ± 3	61 ± 1	55 ± 8	···
IGR J14488-4008	66 ± 9	18.8 ± 1.9⋆	69.7 ± 7.0	···	···	···	2.3
4C +63.22	···	···	10.6 ± 0.1	···	···	···	···
Mrk 1498	47 ± 5	41 ± 4	43 ± 4	130 ± 13	···	81 ± 16	4.9
4C +34.47	203 ± 20	···	493 ± 49	338 ± 17	153 ± 3	117 ± 17	1.0
IGR J17488-2338	132 ± 15	15.5 ± 1.6⋆	53.2 ± 5.3	···	51 ± 1	37 ± 5	3.0
PKS 2014-55	···	···	389 ± 12†	···	···	···	···
4C +74.26	129 ± 13	···	209 ± 21	···	328 ± 13	294 ± 59	8.1
PKS 2331-240	366 ± 37	···	801 ± 80	1110 ± 110	1370 ± 110	1460 ± 390	···
PKS 2356-61	···	···	16 ± 1.6†	···	···	···	>10

Note. First three columns are measurements from TGSS, WENSS, and NVSS surveys, respectively, except starred values at 325 MHz (flux densities from our GMRT campaign) and daggered values at 1.4 GHz (measurements from the literature for PKS 0707-35 and PKS 2356-61, while from SUMSS at 843 MHz for PKS 2014-55). The second three columns are from our Effelsberg 100-m campaign. The last column reports the estimated peak frequency in GHz for sources with a GPS spectral shape. See Section 3.3 for additional measurements from the literature.

previous ones (0318+684, IGR J14488-4008, IGR J17488-2338, and 4C +74.26) show also a convex spectrum, with a minimum at low frequencies with respect to the peak in the GHz range; Callingham et al. (2017) presented a study of sources peaking at low frequencies (<1.4 GHz) by making use of the GLEAM survey (Hurley-Walker et al. 2017). They propose that convex-spectrum sources are undergoing a restarting phase, which is responsible for the peak, while the lower-frequency steep emission should be the remnant of previous activity. Plots of the successfully fitted spectra are presented in Figure 1, while the ones not showing a peak, or that do not have enough measurements for modeling (4C +63.22 and PKS 2014-55), are shown in Figure 2.

Considering the eight sources above, presenting hints of GPS or HFP peaks, and excluding the two sources for which the spectral coverage does not allow us to verify the presence of a peak (4C +63.22 and PKS 2014-55), we obtain a fraction of young radio sources of 61^{+30}_{-21}% (Poissonian errors are considered due to the small number of observed events; Gehrels 1986). Given that these radio cores reside in old radio galaxies, as implied by the large dimensions of their lobes, this high fraction is surprising and difficult to interpret. It is, in fact, hard to compare this fraction with those seen in other samples given the peculiar selection of our sources. Nevertheless, we recall that the frequency of occurrence of the GPS and CSS sources in different flux-density-limited samples ranges from 8 to 10% in the first case and 10%–30% in the second case (depending on the selection frequency; O'Dea 1998 and references therein). More recently, Sadler et al. (2014) examined the radio population at 20 GHz (a frequency dominated by the core emission), which suggests that the combined fraction of GPS/CSS objects can be even higher, reaching values up to 40%, if low-luminosity sources are taken into account. On the other hand, by studying the GLEAM radio source population, Callingham et al. (2017) found that 4.5% of the objects are peaked spectrum sources (GPS/HFP/CSS), thus indicating a large spread in the observed fractions. Furthermore, one must underline that the identification of these radio sources is not straightforward, since on one hand, it requires sufficient spectral data that a peak in the spectrum can be identified, while on the other hand, it is typically limited to the analysis of unresolved, i.e., compact, objects. Thus, the statistical values quoted above are probably lower limits.

To the best of our knowledge, systematic searches for CSS/GPS/HFP objects in the core of extended radio galaxies have never been performed, although a few examples of such objects were previously reported in the literature (O'Dea 1998); this is understandable, since FRI/FRII are thought to be the final stage of peaked spectrum radio sources, but the issue may be reconsidered in view of the evidence that recurrent activity in radio galaxies is indeed observed. Furthermore, such searches should be targeted to radio-selected samples of radio galaxies, whereas our sample is hard-X-ray-selected and is thus likely to pick up objects with active, and thus possibly young, cores.

Considering our own sample of hard-X-ray-selected radio galaxies from Bassani et al. (2016) and limiting the search to objects with small dimensions—36 with dimensions below 200 kpc, which is assumed as the maximum size for intermediate radio galaxies between CSS (<20 kpc) and the most extended ones (>200 kpc)—we could provide a first comparison sample, despite broadband radio data being scarce above 1 GHz, and the AGN core is often radio weak or unresolved with respect to the large radio structure. Indeed, a detailed analysis of the entire sample would require an ad hoc observing campaign and is therefore beyond the reach of the present work. Nevertheless, searching the available literature, we were able to obtain spectral information for 12 of the 36 low-size objects: 2 can be considered to be peaked spectrum objects in the range 150 MHz–10 GHz and are thus similar to the one explored in this work (4C 50.55, Molina et al. 2007; 3C 390.3, Alef et al. 1996), while the other 10 have instead flat or steep spectrum cores (Cygnus A, Carilli & Barthel 1996; 3C 309.1, O'Dea 1998; Pictor A, Perley et al. 1997; 3C 389, Perley & Butler 2017; 3C 382 and 3C 452, Riley & Branson 1973;

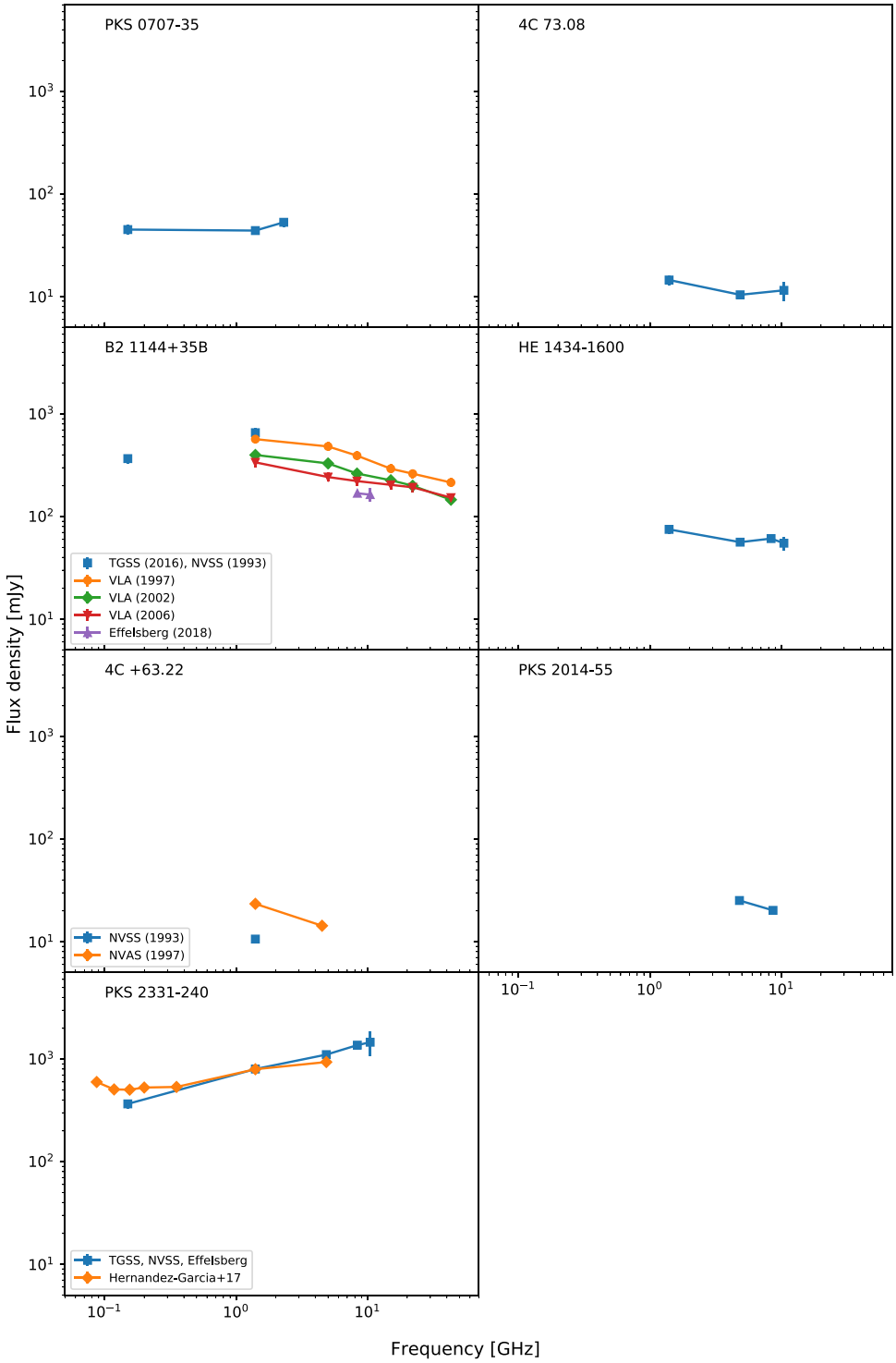

Figure 2. Non-GPS radio cores spectra. Sources 4C +63.22 and PKS 2356-61 do not have enough spectral coverage to exclude the presence of a peak. Errors in the logarithmic scale are smaller than the symbol size for most measurements.

NGC 1275, 3C 120, 3C 184.1, and 3C 227, Healey et al. 2007). This suggests that young cores in our sample can be found in extended radio galaxies of all sizes, but are probably less common in small-sized objects (albeit their fraction has to be properly estimated), giving a first indication that the hard X-ray selection should not have a dominant effect on the abundance of such sources. Nevertheless, only a dedicated observing campaign could exclude it.

All together, and limiting the analysis to our GRG, we find that their cores are mostly young (∼kyr) at radio frequencies, while their structure is old and evolved (∼Myr). From the analysis of their X-ray spectra (Ursini et al. 2018), we also find that the nuclei of these GRG are presently active and powered by a hot corona coupled to an efficient accretion disk. Interestingly, a high-energy cutoff has been measured in four X-ray spectra, and all of these four sources belong to the GPS class. The presence of a high-energy cutoff is a signature of the

X-ray emission originating via thermal Comptonization rather than synchrotron and/or inverse Compton in a jet, implying that the nuclear X-ray emission is not dominated by the jet but rather by the coronal emission of the active nucleus. Finally, a morphological study of the sample (Bruni et al. 2019; G. Bruni et al. 2019, in preparation), as well as the analysis of individual sources (PKS 2331-240, Hernández-García et al. 2017; Mrk 1498, L. Hernández-García et al. 2019, in preparation), also highlights objects with evident signs of restarting activity, further increasing the number of GRG from Bassani et al. (2016) that experienced reactivation of their cores. This finding, together with the abundance of GRG in our sample, supports the scenario originally proposed by Subrahmanyan et al. (1996), in which multiple episodes of activity would favor the growth of radio sources up to the extreme size of GRG.

4.1. Variability

In general, the flux density of the sources in our sample is dominated by extended emission that is not variable, some amount of variability may be foreseen in the nuclear components in case the accretion is not constant, and geometrical effects (reorientation of the radio axis) are favorable. In fact, the symmetry and the size of the GRG implies that the large-scale emission lies roughly in the plane of the sky. The nuclear region (often difficult to disentangle) instead may have been reoriented. Furthermore, in our study, the resolution of the observations may force us to consider also portions of nonvariable jet emission within the core region, which may partially wash out the core variability. With this caveat, we found significant variability for three of them (B2 1144+35B, 4C +63.22, and 4C 34.47) in the core flux density from the literature (B2 1144+35B, see previous section) or by comparing archive and survey data. Indeed, 4C +63.22 shows an increase of a factor of ∼2 at 1.4 GHz in the NVAS data with respect to NVSS (23.4 ± 1.1 mJy versus 10.6 ± 0.1 mJy); NVAS data are from 1997, while NVSS data are from 1993. Analogously, for 4C 34.47, the two NVAS measurements at 15 GHz show a factor of ∼3 decrease in six months, from 1984 November to 1985 May (767 ± 38 mJy versus 226 ± 11 mJy). This source was already studied by Hocuk & Barthel (2010), who estimated a viewing angle of 57° and a core variability up to 25% in 10 yr. Another two sources, B3 0309+411B and 4C 74.26, are known to have a variable core flux density from previous works: the first was presented by Saikia et al. (1984) and de Bruyn (1989), who show an inverted spectrum up to 100 GHz with a variable core flux density, while the latter was investigated by Riley et al. (1989), Pearson et al. (1992), and Konar et al. (2004), who found a variability of ∼50% at 5 GHz over 14 yr.

Short-term flux density variability due to Doppler boosting is typical of sources with the jet base oriented within a few degrees from the observer's line of sight, although it can be found at larger angles (∼40°, Riley et al. 1989). A few percent of variations can be also due to a synchrotron peak quickly moving toward lower frequencies or to a newly ejected component. This could be the case for B3 0309+411, 4C 74.26, and 4C +34.47, which show an inverted or a GPS spectrum, while for 4C +63.22 we do not have enough information to draw any solid conclusions.

5. Conclusions

We carried out a radio observing campaign on a sample of 15 hard-X-ray-selected GRG, aiming at characterizing the spectral shape of their cores from 150 MHz to 10 GHz, and estimate the fraction of young radio sources. The fraction of self-absorbed cores (either GPS- or HFP-like, 61^{+30}_{-21} %) among the cores of these GRG suggests that a restarting event is ongoing, given that these are located at the center of Mpc-scale —and thus evolved—radio structures. Together with the high fraction of GRG found by Bassani et al. (2016) in their parent sample, these findings suggests that hard-X-ray-selected samples of radio galaxies present Mpc-scale radio structures more easily, and moreover, their cores are often undergoing a restarting episode. This result underlines the importance of systematic studies of the core spectra of evolved radio galaxies, in which a nonnegligible fraction of reactivated nuclei could be present.

The capabilities of the next generation of radio (the Square Kilometre Array and Next Generation VLA) and X-ray (the Advanced Telescope for High ENergy Astrophysics) telescopes together with the Low-Frequency Array will make it possible to confirm whether the fraction of restarted nuclei in radio galaxies has a dependence on hard X-ray luminosity or whether it is intrinsically high, through detailed studies of the link between radio and X-ray emission in these unique structures.

G.B. acknowledges financial support under the *INTEGRAL* ASI-INAF agreement 2013-025-R1. L.H.G. acknowledges support from FONDECYT through grant 3170527. This publication has received funding from the European Union's Horizon 2020 research and innovation program under grant agreement No. 730562 (RadioNet). We acknowledge support from a grant PRIN-INAF SKA-CTA 2016. This work is partly based on observations with the 100-m telescope of the MPIfR in Effelsberg. We thank the staff of the GMRT that made these observations possible. GMRT is run by the National Centre for Radio Astrophysics of the Tata Institute of Fundamental Research.

ORCID iDs

G. Bruni https://orcid.org/0000-0002-5182-6289
F. Panessa https://orcid.org/0000-0003-0543-3617
E. Chiaraluce https://orcid.org/0000-0002-4090-1327
A. Kraus https://orcid.org/0000-0002-4184-9372
D. Dallacasa https://orcid.org/0000-0003-1246-6492
A. Bazzano https://orcid.org/0000-0002-2017-4396
L. Hernández-García https://orcid.org/0000-0002-8606-6961

References

Alef, W., Wu, S. Y., Preuss, E., Kellermann, K. I., & Qiu, Y. H. 1996, A&A, 308, 376
Astropy Collaboration, Price-Whelan, A. M., Sipócz, B. M., et al. 2018, AJ, 156, 123
Baars, J. W. M., Genzel, R., Pauliny-Toth, I. I. K., & Witzel, A. 1977, A&A, 61, 99
Bassani, L., Venturi, T., Molina, M., et al. 2016, MNRAS, 461, 3165
Bicknell, G. V., Dopita, M. A., & O'Dea, C. P. O. 1997, ApJ, 485, 112
Bruni, G., Mack, K. H., Salerno, E., et al. 2012, A&A, 542, A13
Bruni, G., Ursini, F., Panessa, F., et al. 2019, arXiv:1902.01657
Callingham, J. R., Ekers, R. D., Gaensler, B. M., et al. 2017, ApJ, 836, 174
Carilli, C. L., & Barthel, P. D. 1996, A&ARv, 7, 1

Condon, J. J., Cotton, W. D., Greisen, E. W., et al. 1998, AJ, 115, 1693
Crossley, J. H., Sjouwerman, L. O., Fomalont, E. B., & Radziwill, N. M. 2008, Proc. SPIE, 7016, 70160O
Dallacasa, D. 2003, PASA, 20, 79
Dallacasa, D., Stanghellini, C., Centonza, M., & Fanti, R. 2000, A&A, 363, 887
de Bruyn, A. G. 1989, A&A, 226, L13
Fanaroff, B. L., & Riley, J. M. 1974, MNRAS, 167, 31P
Fanti, R., Fanti, C., Schilizzi, R. T., et al. 1990, A&A, 231, 333
Gehrels, N. 1986, ApJ, 303, 336
Giovannini, G., Giroletti, M., & Taylor, G. B. 2007, A&A, 474, 409
Giovannini, G., Taylor, G. B., Arbizzani, E., et al. 1999, ApJ, 522, 101
Healey, S. E., Romani, R. W., Taylor, G. B., et al. 2007, ApJS, 171, 61
Hernández-García, L., Panessa, F., Giroletti, M., et al. 2017, A&A, 603, A131
Hernández-García, L., Vietri, G., Panessa, F., et al. 2018, MNRAS, 478, 4634
Hocuk, S., & Barthel, P. D. 2010, A&A, 523, A9
Hurley-Walker, N., Callingham, J. R., Hancock, P. J., et al. 2017, MNRAS, 464, 1146
Intema, H. T., Jagannathan, P., Mooley, K. P., & Frail, D. A. 2017, A&A, 598, A78
Ishwara-Chandra, C. H., & Saikia, D. J. 1999, MNRAS, 309, 100
Jamrozy, M., Konar, C., Machalski, J., & Saikia, D. J. 2008, MNRAS, 385, 1286
Konar, C., Saikia, D. J., Ishwara-Chandra, C. H., & Kulkarni, V. K. 2004, MNRAS, 355, 845
Kuźmicz, A., Jamrozy, M., Bronarska, K., Janda-Boczar, K., & Saikia, D. J. 2018, ApJS, 238, 9
Laing, R. A., Riley, J. M., & Longair, M. S. 1983, MNRAS, 204, 151
Machalski, J., Chyzy, K. T., & Jamrozy, M. 2004, AcA, 54, 249
Malizia, A., Landi, R., Molina, M., et al. 2016, MNRAS, 460, 19
Marecki, A. 2004, in Proc. of the 7th Symp. of the European VLBI Network on New Developments in VLBI Science and Technology, ed. R. Bachiller et al., 117
Mauch, T., Murphy, T., Buttery, H. J., et al. 2003, MNRAS, 342, 1117
McConnell, D., Sadler, E. M., Murphy, T., & Ekers, R. D. 2012, MNRAS, 422, 1527
Molina, M., Bassani, L., Malizia, A., et al. 2014, A&A, 565, A2
Molina, M., Giroletti, M., Malizia, A., et al. 2007, MNRAS, 382, 937
Molina, M., Venturi, T., Malizia, A., et al. 2015, MNRAS, 451, 2370
Morganti, R., Killeen, N. E. B., & Tadhunter, C. N. 1993, MNRAS, 263, 1023
Morganti, R., Oosterloo, T. A., Reynolds, J. E., Tadhunter, C. N., & Migenes, V. 1997, MNRAS, 284, 541
Müller, P., Krause, M., Beck, R., & Schmidt, P. 2017, A&A, 606, A41
Murgia, M., Fanti, C., Fanti, R., et al. 1999, A&A, 345, 769
O'Dea, C. P. 1998, PASP, 110, 493
O'Dea, C. P., Baum, S. A., & Stanghellini, C. 1991, ApJ, 380, 66
Orienti, M., Dallacasa, D., Tinti, S., & Stanghellini, C. 2006, A&A, 450, 959
Owsianik, I., & Conway, J. E. 1998, A&A, 337, 69
Parma, P., Murgia, M., Morganti, R., et al. 1999, A&A, 344, 7
Pearson, T. J., Blundell, K. M., Riley, J. M., & Warner, P. J. 1992, MNRAS, 259, 13P
Perley, R. A., & Butler, B. J. 2017, ApJS, 230, 7
Perley, R. A., Roser, H.-J., & Meisenheimer, K. 1997, A&A, 328, 12
Phillips, R. B., & Mutel, R. L. 1980, ApJ, 236, 89
Rengelink, R. B., Tang, Y., de Bruyn, A. G., et al. 1997, A&AS, 124, 259
Riley, J. M., & Branson, N. J. B. A. 1973, MNRAS, 164, 271
Riley, J. M., Warner, P. J., Rawlings, S., et al. 1989, MNRAS, 236, 13P
Sadler, E. M., Ekers, R. D., Mahony, E. K., Mauch, T., & Murphy, T. 2014, MNRAS, 438, 796
Saikia, D. J., Shastri, P., Sinha, R. P., Kapahi, V. K., & Swarup, G. 1984, JApA, 5, 429
Saripalli, L. 2007, in PoS, 130
Saripalli, L., Malarecki, J. M., Subrahmanyan, R., Jones, D. H., & Staveley-Smith, L. 2013, MNRAS, 436, 690
Stanghellini, C., O'Dea, C. P., Baum, S. A., et al. 1997, A&A, 325, 943
Subrahmanyan, R., Saripalli, L., & Hunstead, R. W. 1996, MNRAS, 279, 257
Tuccillo, D., Bruni, G., DiPompeo, M. A., et al. 2017, MNRAS, 467, 4763
Ursini, F., Bassani, L., Panessa, F., et al. 2018, MNRAS, 481, 4250
van Breugel, W., Miley, G., & Heckman, T. 1984, AJ, 89, 5
Wilkinson, P. N., Polatidis, A. G., Readhead, A. C. S., Xu, W., & Pearson, T. J. 1994, ApJL, 432, L87